Structural Analysis of Humins Formed in the Brønsted Catalyzed Dehydration of Fructose

Ziwei Cheng[1,2], Jeffrey L. Everhart[2], George Tsilomelekis[2,§], Vladimiros Nikolakis[2,#], Basudeb Saha[2], and Dionisios G. Vlachos[1,2,*]
[1]Department of Chemical and Biomolecular Engineering
[2]Catalysis Center for Energy Innovation
University of Delaware, Newark, DE 19716, USA
[§]Present Address: Chemical and Biochemical Engineering, Rutgers University,
98 Brett Road, Piscataway, NJ 08854, USA
[#] Present Address: W. L. Gore and Associates Inc., 101 Lewisville Rd, Elkton MD 21921, USA

Supplementary Information

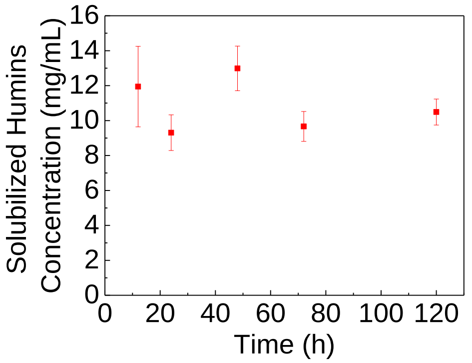

Figure S1. Solubilized humins concentration in ACN as a function of time. 0.45 g humins were mixed with 3 mL of ACN and stirred at room temperature at 1000 rpm. Three replicates were done for each time point.

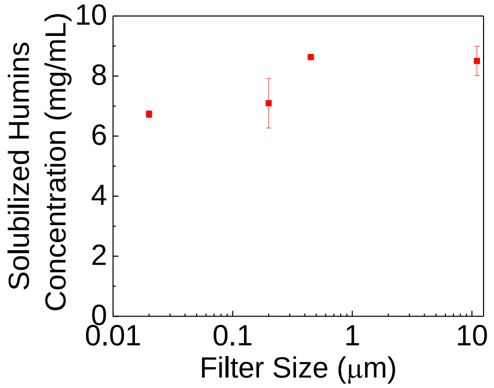

Figure S2. Solubilized humins concentration in ACN as a function of the pore size of the filter. 0.45 g humins were mixed with 3mL of ACN and stirred at room temperature at 1000 rpm.

Vacuum filtration couldn't be used with 0.02, 0.2 and 0.45 µm pore sized filters, so a different procedure was used to investigate the effect of filter pore size. The slurry was filtered using syringe filters of pore sizes 0.02, 0.2, 0.45, and 11 µm. A known amount of filtrate was transferred into a pre-weighed glass vial and put into the vacuum oven at room temperature for 24 h. Subsequently, the vial containing the residue was weighed again. The concentration of solubilized humins was calculated as the mass of the residue divided by the volume of the solvent put into the vial. Three replicates were done for each condition. The concentration of solubilized humins using the 11 µm filter determined using this method is 1-2 mg/mL less than that determined by vacuum filtering the slurry and weighing the undissolved humins.

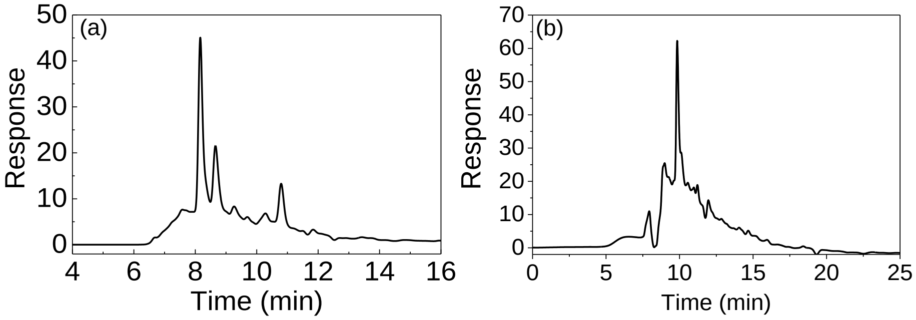

Figure S3. HPLC chromatogram for humins in (a) acetonitrile (ACN) solution and (b) methanol solution. The diode array detector (DAD) was set at 254 nm.

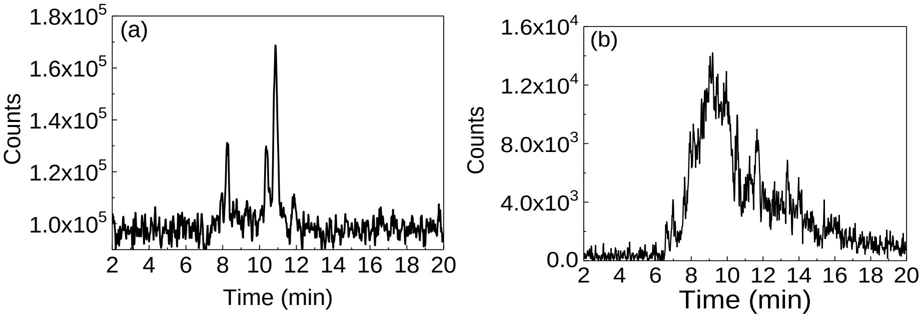

Figure S4. Total ion chromatogram of humins in acetonitrile solution. (a) 10-300 m/z. (b) 301-500 m/z.

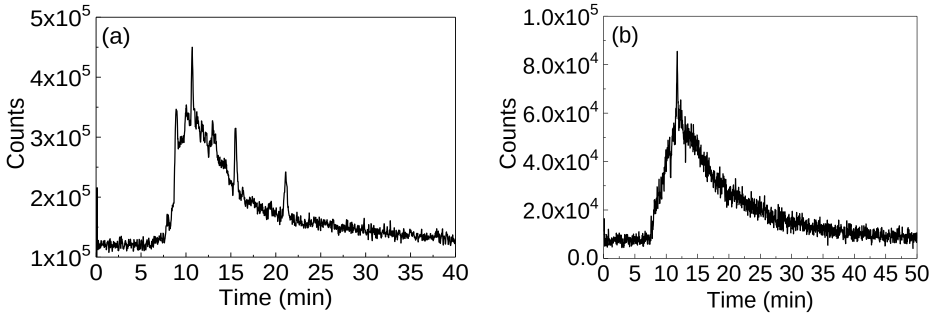

Figure S5. Total ion chromatogram of humins in methanol solution. (a) 10-600 m/z. (b) 601-1200 m/z.

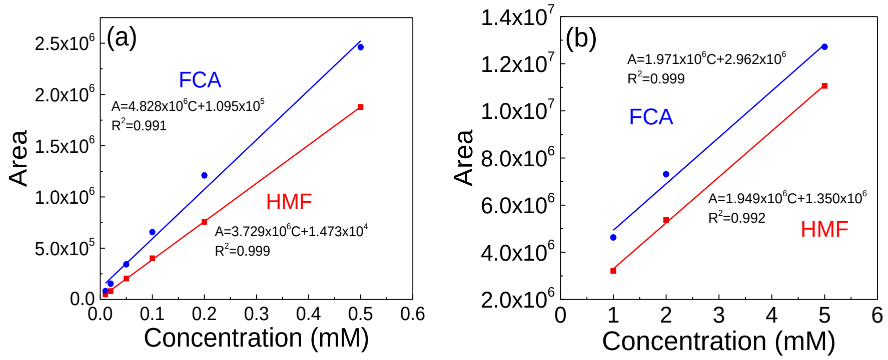

Figure S6. Calibration plots of 2-(4-formylphenoxymethyl) furan-3-carboxylic acid (FCA) and HMF (a) 0-0.5 mM and (b) 1-5 mM in acetonitrile.

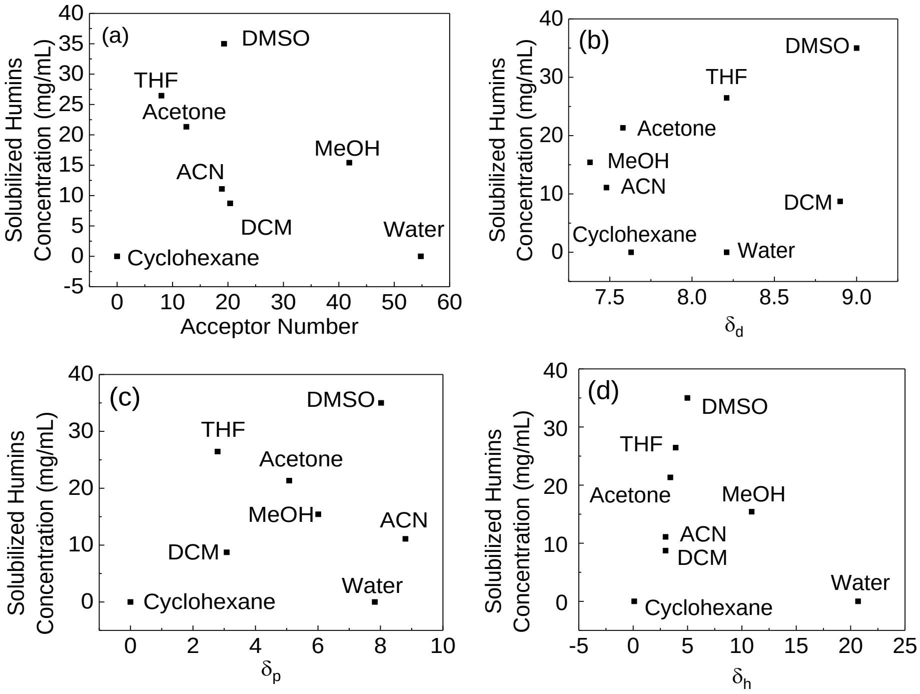

Figure S7. Solubilized humins concentration versus solvent properties. (a) Acceptor number (AN), (b)~(d) Hansen solubility parameters δ_d, δ_p, and δ_h. No clear correlation between the solubilized humins concentration and AN, δ_d, δ_p, or δ_h was found.

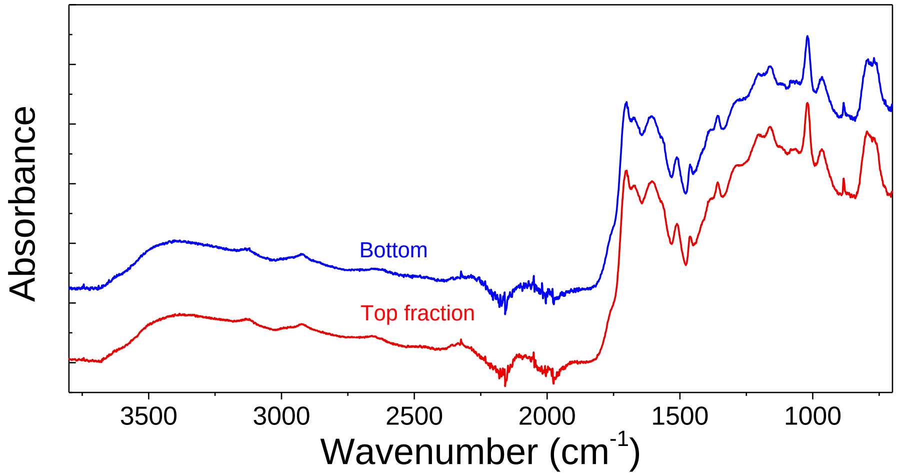

Figure S8. FTIR spectra of humins floating on top and settling to the bottom when placed in water. The nearly identical spectra indicate these fractions have the same chemical structure but are inhomogeneous in density.

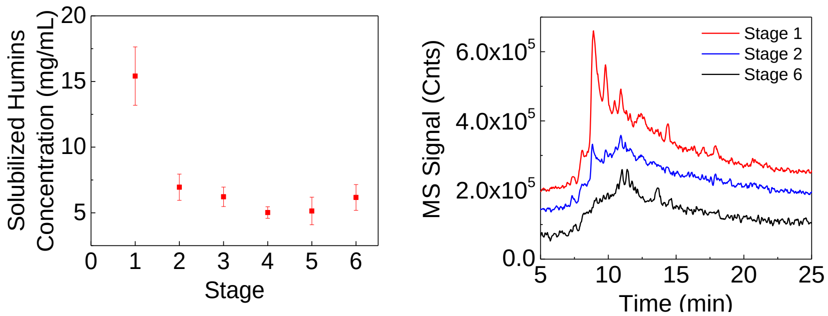

Figure S9. (a) Concentration of the methanol solubilized humins at stages 1-6. 0.45 g of insoluble humins obtained from the previous stage was mixed with 3 mL of methanol and stirred at 25 °C for 24 h at 1000 rpm. The number of replicates was 10 at the first stage and decreased to 3 at the 6th stage. (b) Total ion chromatogram (TIC) of methanol solubilized humins for stages 1, 2, and 6 at 10-600 m/z.

Table S1. Concentrations of dominant species of solubilized humins detected by LC-MS.

ACN solvent	Methanol solvent

Commented [CZ1]: Reviewer 3, Comment 4: Table 1 that was previously in the main text was moved to Supplemental Information as Table S1.

Mass (m/z)	Concentration (mM)	Mass (m/z)	Concentration (mM)
99	2.80	99	1.42
109	0.54	127	1.76
127	6.48	141	16.4
217	0.24	195	0.35
225	0.66	185	1.87
235	3.88	239	0.42
252	1.54	235	0.18
207	0.61	249	0.30
151	0.05	295	0.69
219	0.14	349	1.23
191	0.28	219	0.46
315	0.31	303	0.41
343	0.37	340	0.48
247	0.19	679	0.04
241	0.11	701	0.03

Table S2. Concentrations of prevalent, MeOH soluble humins masses of Soxhlet extracted and manually washed humins.

Mass (m/z)	Manually Washed Humins (mM)	Soxhlet Extracted Humins (mM)
99	1.42	0.19
127	1.76	0.22
141	16.36	0.94
195	0.35	0.11
185	1.87	0.13
239	0.42	0.13
235	0.18	0.07
249	0.30	0.09
295	0.69	0.11
349	1.23	0.18
219	0.46	0.12
303	0.41	0.44

340	0.48	0.26
679	0.04	0.05
701	0.03	0.04

Table S3. Mole percentage (%) of each mass in the total amount of monitored species, determined by LC-MS analysis.

m/z	Stage 1	Stage 2	Stage 3	Stage 4	Stage 5	Stage 6
99	15.37	4.49	6.92	10.56	13.19	16.82
109	2.96	4.18	3.91	4.56	4.88	3.99
127	35.58	8.19	14.67	19.49	17.22	26.79
217	1.32	3.55	4.00	3.69	4.31	3.23
225	3.61	5.35	4.76	4.06	5.53	4.58
235	21.30	8.59	16.01	8.39	7.99	6.13
252	8.45	37.77	21.56	16.98	12.04	7.73
207	3.38	3.28	3.68	4.96	6.04	4.92
151	0.29	0.79	1.03	1.49	1.75	2.46
219	0.79	7.60	3.61	3.61	3.00	0.00
191	1.56	5.38	7.76	11.11	11.93	12.35
315	1.70	3.31	3.80	3.25	3.35	2.97
343	2.04	3.89	3.98	3.30	3.30	3.05
247	1.04	2.22	2.66	3.06	3.77	3.71
241	0.62	1.41	1.65	1.48	1.70	1.27

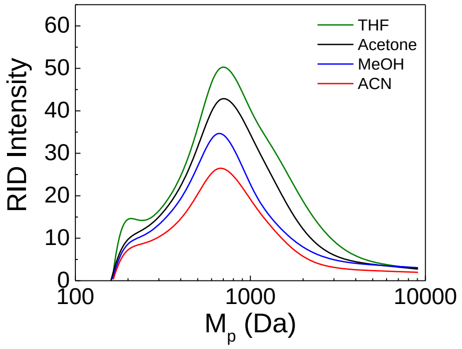

Figure S10. Refractive index detector (RID) intensity as a function of molecular weight for the acetone, ACN, methanol, and THF solubilized humins. Here the humins did not undergo Soxhlet extraction before dissolution in organic solvents.

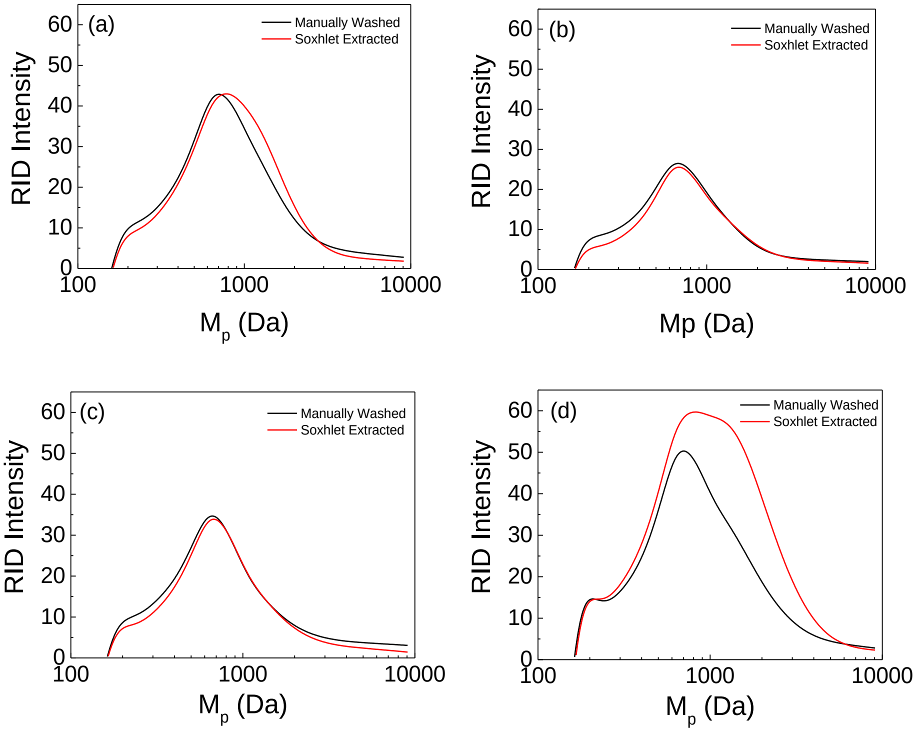

Figure S11. Molecular weight distribution for the (a) acetone, (b) acetonitrile, (c) methanol, and (d) THF-soluble portions of humins that were Soxhlet extracted (red) and only manually washed with DI water before dissolution (black).

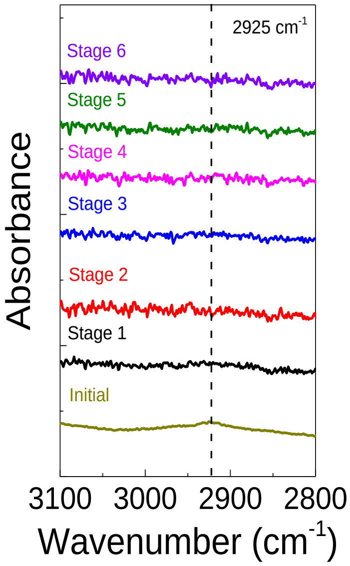

Figure S12. Zoomed in of the high wavenumber region of Figure 4a showing the 2925 cm^{-1} (C-H stretching) peak for the initial humins and the decreasing intensity of this peak in the insoluble humins from dissolution stages 1~6.

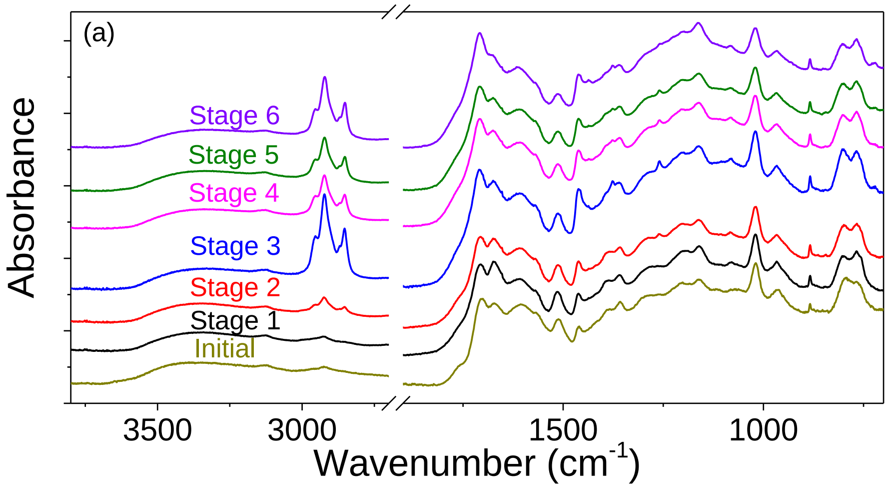

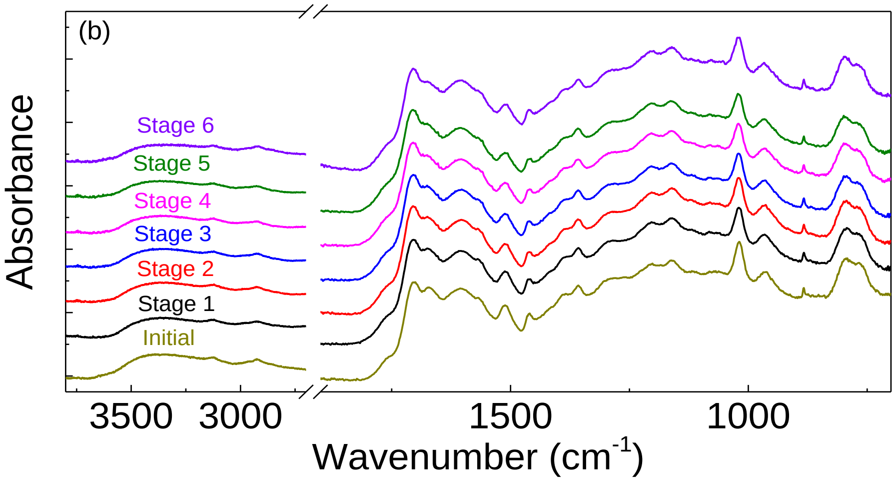

Figure S13. FTIR spectra of initial humins, and (a) the methanol solubilized humins at each stage of dissolution, and (b) insoluble humins remaining after each stage of dissolution.